Theor Chem Account (2008) 120:557–564
DOI 10.1007/s00214-008-0434-7

REGULAR ARTICLE

Elastic and dynamical properties of alkali-silicate glasses from computer simulations techniques

Alfonso Pedone · Gianluca Malavasi · Alastair N. Cormack · Ulderico Segre · M. Cristina Menziani

Received: 26 September 2007 / Accepted: 25 February 2008 / Published online: 12 March 2008

Abstract This paper shows recent progresses in the field of computer simulations of inorganic glasses. Molecular dynamics simulations and energy minimization methods have been applied to calculate the elastic and transport properties of alkali silicate glasses of compositions $x\mathrm{M_2O} \cdot (100 - x)\mathrm{SiO_2}$ (with $x = 0$, 10, 15, 20, 25, 30 % mol for M = Li, Na and K) and of a soda-lime glass with composition $15\mathrm{Na_2O} \cdot 10\mathrm{CaO} \cdot 75\mathrm{SiO_2}$, which has been employed to ascertain the effect of the replacement of CaO for $\mathrm{Na_2O}$. The excellent agreement of the computed results with the experimental data highlights the important predictive and interpretative role reached by computer simulations techniques.

1 Introduction

Alkali silicate and soda-lime glasses are the prototype of a variety of multicomponent industrial and natural glasses.

The complexity of silicate glasses is well known. Advanced techniques such as X-ray absorption fine structure (XAFS), [1,2], magic angle spinning NMR (MAS-NMR) [3–9] and neutron diffraction [10–14] together with molecular dynamics simulation techniques [4,15–23] have been crucial in the elucidation of the detailed short and medium range order structure.

From such techniques, a model known as the modified random network (MRN) has emerged. This successfully accounts for the structural properties of silicate glasses [24]. According to the MRN model, the continuous random network of bridged $\mathrm{SiO_4}$ units in pure silica is significantly altered by the modifying cations (e.g. Li, Na, K, etc.), which, through the process of micro-segregation, cluster in proximity of the bridged $\mathrm{SiO_4}$ units to which they are linked predominantly via the non-bridging oxygens atoms. At high concentrations, the modifiers percolate through the bulk of the glass and form primary pathways, or channels, which play a key role in the elastic and transport properties of glasses.

Since mechanical strength, chemical durability and conductivity [25] often dictate whether a specific need or application can be met, the prediction of these properties according to glass composition is becoming increasingly indispensable to develop materials with a greater focus on end-user application requirements, reduction of development costs and decreasing time to market.

This paper shows that computational simulations are invaluable tools for obtaining both correct numerical estimations of the mechanical and transport properties of interest and atomistic three-dimensional models for the interpretation of the variation of the observed properties.

2 Computational methods

2.1 Simulation procedure

The structures of alkali-silicate glasses of composition $x\mathrm{M_2O} \cdot (100 - x)\mathrm{SiO_2}$ (with $x = 0$, 10, 15, 20, 25, 30 mol % for M = Li, Na and K) and a soda-lime glass of composition $15\mathrm{Na_2O} \cdot 10\mathrm{CaO} \cdot 75\mathrm{SiO_2}$ have been modelled by means of NVT molecular dynamics (MD) simulations. For each

Contribution to the Nino Russo Special Issue.

A. Pedone · G. Malavasi · U. Segre · M. C. Menziani (✉)
Dipartimento di Chimica, Università di Modena e Reggio Emilia, Via G. Campi 183, 41100 Modena, Italy
e-mail: menziani@unimo.it

A. N. Cormack
Kazuo Inamori School of Engineering, New York State College of Ceramics, Alfred University, Alfred, NY 14802, USA

Table 1 Molar composition, number of atoms, densities and cell sizes of the $xM_2O-(100-x)SiO_2$ simulated glasses (M = Li, Na, K) and soda-lime glass

Formulation	xM_2O (mol %)	Density (g/cm^3)	Cell size (Å)
SiO_2	0	2.200	28.5290
LS10	10	2.246	27.8519
LS15	15	2.269	27.5066
LS20	20	2.292	27.1694
LS25	25	2.314	26.8245
LS30	30	2.334	26.4848
NS10	10	2.294	28.1633
NS15	15	2.340	27.9924
NS20	20	2.385	27.8294
NS25	25	2.428	27.6788
NS30	30	2.469	27.5393
KS10	10	2.305	28.6087
KS15	15	2.347	28.6935
KS20	20	2.390	28.7611
KS25	25	2.429	28.8512
KS30	30	2.466	28.9454
N15C10S	$15Na_2O \cdot 10CaO \cdot 75SiO_2$	2.466	28.9454

The total number of atoms in each box is 1,536 for alkali silicate glasses and 1,450 for the soda-lime glass

composition, 1,536 atoms were placed randomly in a cubic box; three simulations were carried out with different starting configurations. Atomic compositions and size length of the simulation boxes are reported in Table 1, together with the glass densities at room temperature calculated according to Appen's empirical method [26].

The DL_POLY [27] package has been employed for MD simulations. Integration of the equation of motion has been performed using the Verlet Leap-Frog algorithm with a time step of 2 fs. Coulombic interactions have been calculated by the Ewald summation method [28] with a cut-off of 12 Å and an accuracy of 10^{-4}. The short range interaction cut-off was set to 5.5 Å.

A pair-wise potential recently developed by us has been employed. [29]. This is based on a rigid ionic model, with partial charges to handle the partial covalency of silicate systems. The potential is given by the sum of three terms: (1) the long-range Coulombic potential; (2) the short-range forces, which are represented by a Morse function; (3) an additional repulsive term C/r^{12}, which has been added to model the repulsive contribution at high-temperature and pressure. The expression for the model potential is:

$$U(r) = \frac{z_i z_j e^2}{r} + D_{ij} \times \left[\left\{1 - \exp\left[-a_{ij}(r - \bar{r}_{ij})\right]\right\}^2 - 1\right] + \frac{C_{ij}}{r^{12}} \qquad (1)$$

where $z_i, z_j, D_{ij}, a_{ij}, \bar{r}_{ij}$ and C_{ij} are parameters and the indices i and j refer to the different atomic species. The atomic charge for an alkali ion is assumed to be $q = +0.6$ e, and the values of z_i for the other atoms are taken accordingly. The values of the other parameters in Eq. 1 are listed in Table 2. They were derived by fitting both structural and mechanical properties of inorganic oxides according to the procedure implemented in the GULP code [30].

As in previous works which employed a rigid ionic model with partial charges, [29,31,32] the systems have been cooled down uniformly from 5,000 to 300 K, by decreasing the temperature in steps of 500 K. The total cooling time is 470 ps with 235×10^3 time steps and a nominal cooling rate of 1×10^{13} K/s. At each temperature a 20,000 time steps relaxation has been allowed. During the first set of 6,000 time steps, the velocity is scaled every time step. During the second set of 6,000 time steps, velocity scaling every 40 time steps has been performed, and finally, during the last 8,000 time steps, no velocity scaling was applied. Data collection has been performed every 50 time steps during the last 15,000 of 35,000 time steps using the micro-canonical ensemble NVE.

2.2 Elastic properties

The elastic properties of the glasses have been computed by means of the static method. In this method the structures are optimized via energy minimization and the elastic properties are calculated from the curvature of the energy surface at the minimum [33].

Table 2 Potential parameters for Eq. (1)

	D_{ij} (eV)	a_{ij} (Å^{-1})	$\bar{r}_{ij}$ (Å)	C_{ij} (eV·Å^{12})
$Li^{0.6} - O^{-1.2}$	0.001080	3.429361	2.680018	1.0
$Na^{0.6} - O^{-1.2}$	0.023363	1.763867	3.006315	5.0
$K^{0.6} - O^{-1.2}$	0.011612	2.062605	3.305308	5.0
$Si^{2.4} - O^{-1.2}$	0.340554	2.006700	2.100000	1.0
$O^{-1.2} - O^{-1.2}$	0.042395	1.379316	3.618701	100.0

The stiffness matrix elements for a crystalline system are defined as the second derivative of the energy (U) with respect to the strains (ε):

$$C_{ij} = \frac{1}{V}\left(\frac{\partial U}{\partial \varepsilon_i \partial \varepsilon_j}\right) \tag{2}$$

Once the stiffness matrix **C** is obtained, the Young's modulus values along three principal directions can be obtained by:

$$E_k^{-1} = S_{kk} \quad (k = 1,\ 3). \tag{3}$$

where S_{kk} are the elements of the compliance matrix, which is the inverse of the stiffness matrix, $\mathbf{S} = \mathbf{C}^{-1}$. For isotropic materials the three principal values must be equal.

The elastic properties have been computed for the glasses obtained from the MD simulation runs by means of the GULP code [30]. A Newton–Raphson [34] energy minimization has been performed at constant pressure (1 atm). The coulomb term has been evaluated by means of the Ewald method in which the real cut-off has been determined according to an accuracy of 10^{-8} [35]. The minimum image convention has been turned off and the short-range potentials cut-off has been set to 10 Å. The approach of Fletcher and Powell [36] has been used to update the Hessian matrix. To handle the amorphous character of the glass a cubic cell with no symmetry (space group $P1$) has been used as MD simulation cell.

2.3 Dynamical properties

The dynamical properties of the glasses studied have been determined in the range 1,000–2,600 K. For each system the configuration obtained by MD simulation at 300 K has been reheated using the Beredsen barostat [37] with frictional constants set to 0.4 ps. At each temperature the systems have been relaxed for 40 ps followed by 2 ns of data production. Configurations were saved at intervals of 0.1 ps and used subsequently to calculate dynamical properties.

The mean square displacement $\sigma_j(t)$ measures the average distance an atom of the jth species travels in the time t and it is defined according to the following equation:

$$\sigma_j(t) = \frac{1}{N_j}\sum_{i=1}^{N_j}\left\langle \Delta \mathbf{r}_i(t)^2 \right\rangle = \frac{1}{N_j}\sum_{i=1}^{N_j}\left\langle (\mathbf{r}_i(t) - \mathbf{r}_i(0))^2 \right\rangle \tag{4}$$

where $\mathbf{r}_i(t) - \mathbf{r}_i(0)$ is the (vector) distance travelled by atom i over some time intervals of length t, and the squared magnitude of this vector is averaged over many such time intervals and over all atoms of the jth species in the system.

The limiting slope of $\sigma_j(t)$, considered for time intervals sufficiently long for it to be in the linear regime, is related to the self-diffusion constant D_j by the Einstein relation:

$$D_j = \frac{1}{6}\lim_{t\to\infty}\frac{d}{dt}\sigma_j(t) \tag{5}$$

3 Results and discussion

3.1 Structure

Structural features representing short and medium range order have been deeply discussed in a previous work in which good agreement between the results of computer simulations and neutron diffraction was found [33]. Therefore, we summarize here only the main features concerning short and medium range order that affect the elastic properties.

Different short range order has been found for lithium, sodium and potassium ions. Lithium shows an average coordination number of 3.0 and a distance of 1.968 Å for Li–NBO (NBO: non-bridging oxygen) and an average Li–BO (BO: bridging oxygen, which are bonded by two silicons) coordination number of 0.9 associated to a distance of 2.090 Å. The Na–O bond lengths range from 2.300 to 2.332 Å, which compare well with EXAFS and neutron diffraction data of 2.30 – 2.36 Å [2,38,39]. The coordination number of the sodium ions increases from 4.8 to 5.3 for the NS10 and NS30 glasses. Similarly, EXAFS studies by Greaves et al. [39] show a coordination number of 5 ±0.5 for the Na ions in sodium di-silicate glasses. The K–O bond length values range between 2.687 and 2.724 Å with a coordination number of 7.6 for all the compositions studied.

The different short range order around the three alkaline ions studied leads to the different medium range order of the

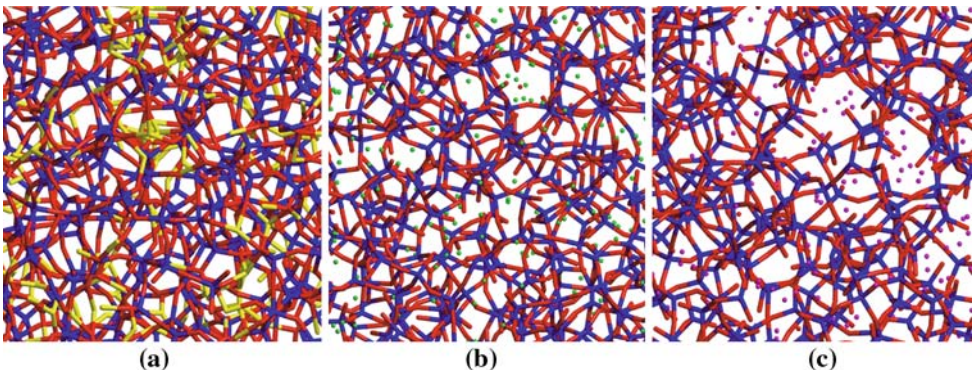

Fig. 1 Structural changes in the glass network encountered by addition of Li (*light yellow*), Na (*light green*) and K (*light magenta*) ions. Silicon and oxygen are represented as *blue* and red *sticks*, respectively. **a** LS25 glass network (Li is fourfold coordinated and seems to act as a network former increasing the polymerization and packing of the structure. Because of its small size and high field strength Li shows an high degree of ions clustering and forms small rings), **b** NS25 glass network (the Na ion is fivefold coordinated and acts as a modifier disrupting the silica network), **c** KS25 glass network (the K ion is 7–8-fold coordinated, its big size causes the formation of large rings and wide percolation channels are found)

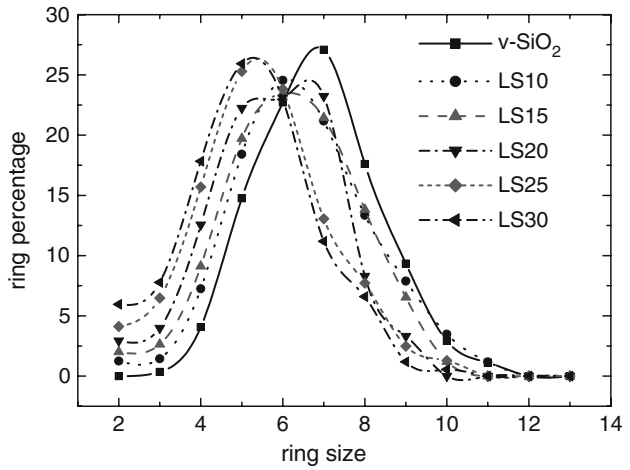

Fig. 2 Ring size distribution for lithium silicate glasses calculated by considering Li as pseudo-network former. Adding Li_2O the maximum shifts to smaller rings leading to a greater overall cross-linking of the network

glasses studied. A visual inspection of the MD-derived glass structures presented in Fig. 1 shows that Li addition to silica glass leads to an increasing cross-linking and cohesion of the network. In this context, lithium seems to act as a 'pseudo-network former' with fourfold coordination and high force constant. On this basis an accurate evaluation of the network polymerization can be obtained by the ring size distribution for lithium silicate glasses reported in Fig. 2; in this analysis Li has been considered as network former. A significant shift of the maximum in the ring size curve to smaller rings as a function of Li concentration is observed.

Because of their higher coordination numbers, longer distances and lower force constants Na and K act as purely modifier cations. They create bigger percolation channels depending on the modifier sizes, the potassium silicate glasses having the more depolymerized network structure and largest channels.

The analysis of the soda-lime glass shows that Ca ion is six fold coordinated by 4.5 NBO, and 1.5 BO, respectively, forming a reasonably regular octahedron. Therefore, Ca seems to play a similar, modifying, role as sodium in the structure as shown in Fig. 3 and recently discussed by Cormack and Du [40].

3.2 Elastic properties

The data values of the elastic properties are obtained as the average over three simulation runs. Slightly different values of the Young's modulus E in three orthogonal spatial directions result from the simulations because of clustering of specific ions at the atomic scale. This phenomenon has been outlined previously both from computer simulations studies [4,15,41] and experimental measurements [24]. However, since the E values calculated along the three directions differ by less than 10%, the Young's modulus is calculated as their average.

Table 3 lists the computed Young's modulus of the alkali silicate glass compositions, together with the experimental data available from literature [42]. It is worth noticing that for lithium silicate systems with small lithium content NMR experiments show that clustering of Li-rich regions is observed [4]. This clustering is reproduced in the present work, however, the dimensions of the box used do not allow a detailed analysis as was done previously [41]. This clustering seems to increase the differences of the Young's modulus among the three directions, in fact the greatest difference of 15% was found in the case of LS10 glass. At low alkali content the degree of isotropy follows the trend K-glasses

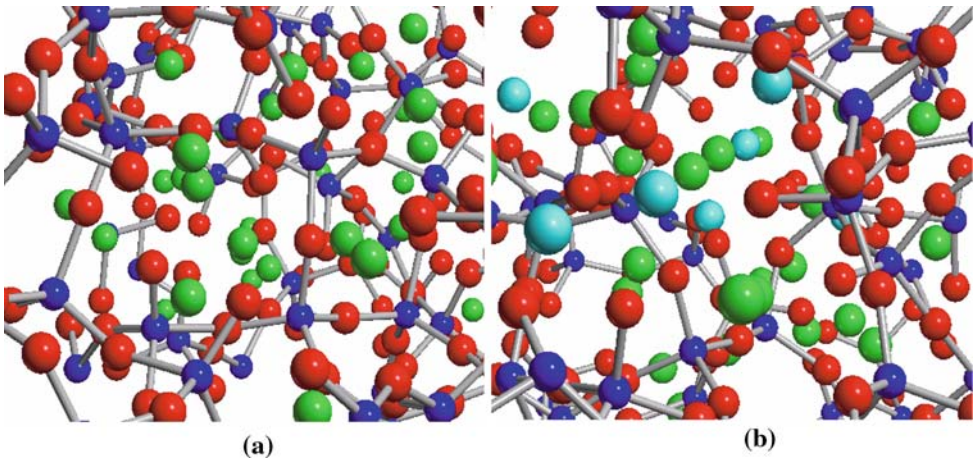

Fig. 3 **a** Snapshot of channels created by Na ions (*light green*) of the NS25 glass and **b** channels created by Ca (*light cyan*) and Na (*light green*) of the N15C10S glass

Table 3 Young's modulus for lithium, sodium and potassium silicate glasses and soda lime glass computed with Pedone's Force Field from Ref. [29] (FF), Priven 2000 empirical method [43] and experimentally measured [54]

xM_2O (mol %)	Experimental data			FF			Priven 2000		
	Li	Na	K	Li	Na	K	Li	Na	K
E (GPa)									
0	72.50	72.50	72.50	72.05 (−0.6)	72.05 (−0.6)	72.05 (−0.6)	68.00 (−6)	68.00 (−6)	68.00 (−6)
10	74.26	65.29	–	75.46 (2)	64.20 (−2)	56.00	70.80 (−5)	59.30 (−9)	59.30
15	76.42	62.90	52.67	73.30 (−4)	61.07 (−3)	53.62 (2)	72.20 (−6)	62.45 (−0.7)	54.95 (4)
20	76.99	61.08	49.04	76.16 (−1)	58.53 (−4)	49.42 (0.8)	73.60 (−4)	60.60 (−0.8)	50.60 (3)
25	78.44	59.77	46.45	78.52 (0.1)	58.13 (−3)	46.59 (0.3)	75.00 (−4)	58.75 (−2)	46.25 (−0.4)
30	78.81	59.33	–	78.74 (−0.1)	56.64 (−4)	42.56	76.40 (−3)	56.90 (−4)	41.90
N15C10S	68.4			67.2 (−1.8)			69.7 (1.9)		

The percent errors with respect to experimental data are reported in brackets. Elastic constants for SiO_2 glass ($x = 0$) and the N15C10S glass have been taken from Refs. [55,56]

> Na-glasses > Li-glasses with the greater differences of 7.5, 13.0 and 13.0% for the KS15, NS15 and LS15 glasses, respectively. With the addition of modifiers the degree of isotropy increases in the case of lithium and sodium silicate glasses, the greater differences along the three directions being 8 and 10% in both cases.

Comparison with the results obtained by means of several empirical models available in the SciGlass package [26] has also been performed. Table 3 lists the results obtained with the Priven 2000 method [43] which furnishes the best experimental data predictions. This is an incremental model where chemical equilibrium factors are derived from the properties of binary and ternary glasses and various property equations are applied, depending on the glass composition and temperature.

Overall good agreement with the experimental data is obtained. No experimental errors are associated with the data values taken from literature, however, being obtained by ultrasonic wave propagation they are assumed to be quite accurate. The computed Young's modulus values are reproduced with maximum differences with respect to the experimental value of 4, 4 and 2% for lithium, sodium and potassium silicate glasses, respectively. Almost all the elastic properties values predicted with the Priven 2000 empirical method are underestimated and maxima differences below 5, 9 and 4% have been found for lithium, sodium and potassium silicate glasses, respectively.

Despite the great advantage of obtaining a rough estimate of the mechanical properties with a very low computational effort with respect to atomistic simulation techniques, the Priven method does not provide insight into the atomistic structural and dynamical features responsible for the variation of the observed properties. This interpretative aspect is, on the contrary, the main advantage of the atomistic simulations.

It is usually believed that, because of their modifier nature, the addition of alkali oxides to silica glass results in a decreasing of the glass Young's modulus values. In fact, the addition of one network modifier unit M_2O causes one BO bridging between two connected tetrahedra to be replaced by two NBO's, one on each tetrahedron. The presence of NBO determines a break in the linkage within the structure and, therefore, favours the displacements of the atoms. On this

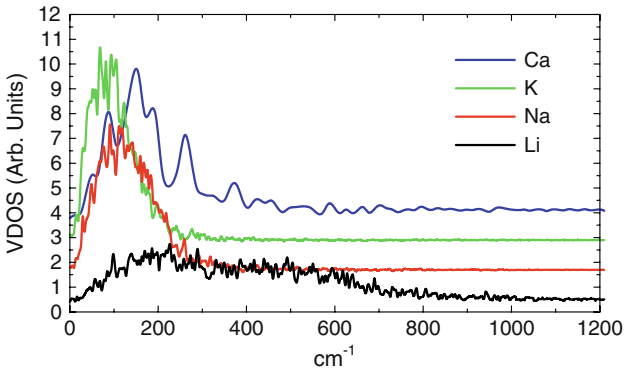

Fig. 4 Projection of VDOS for each different modifier of the glasses LS15 (*black line*), NS15 (*red line*) and KS15 (*green line*) and Ca ions in N15C10S (*blue line*). The plots have been shifted vertically for the sake of clarity

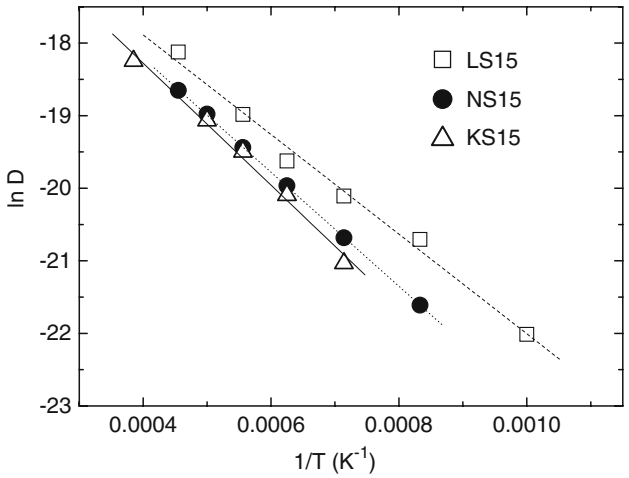

Fig. 5 Arrhenius plots of the diffusion coefficients for the three different $15M_2O \cdot 85SiO_2$ glasses

basis, one should expect E to be directly proportional to the total number of Si–O–Si bridges. However, the results show that this is not the case. In fact, the average percentage of Si–O–Si bridges is not influenced by the chemical nature of the alkali ions.

Vallis et al. [44] claimed that the variation in the values of the elastic moduli of alkali silicate glasses might be the result of two opposite effects: (a) the depolymerization of the SiO_2 network by the modifiers addition would decrease the cohesion of the SiO_2 chains and consequently would lead to a decrease of the elastic constants; (b) the establishment of new NBO–M–NBO or NBO–M–BO interactions (with M = cation modifier) would promote the cohesion of the glass leading to an increase in the elastic constants as a function of the concentration of the modifiers.

It is therefore necessary to understand which of these effects dominates in the systems studied. The strength of the cation modifier oxygen bond is not easily determined in a glass; however, a semi-quantitative estimate of the strength of chemical bonds between cations and the surrounding oxygen atoms in the simulated glasses is obtained by the evaluation of force constants via vibrational frequencies.

Figure 4 shows the projection of the vibrational density of states (VDOS) for Li, Na and K ions. The projection of VDOS for Na and K has a log-normal shape, the K one being narrower and shifted to lower frequencies. The K–O frequencies range from 30 to 170 cm^{-1} with a maximum peak at 97 cm^{-1}, the Na–O frequencies range from 50 to 250 cm^{-1} with a maximum at 130 cm^{-1}. Li VDOS is spread out over a larger frequency interval which ranges from 100 to 700 cm^{-1}, with two peaks at around 240 and 500 cm^{-1} .

These results agree well with far infrared spectra which exhibit a band, named "cation mode", characteristic of the interaction between alkali atoms and the NBO atoms in the glass network. The frequency of this band is weakly dependent on the nature of the network forming ion (Si, V, B, P, and Ge) but it is strongly dependent on the nature of the modifier cations [45]. The experimental values are: $\overline{\nu}_{Li-O} = 347\,cm^{-1}\overline{\nu}_{Na-O} = 180\,cm^{-1}$ $\overline{\nu}_{K-O} = 113\,cm^{-1}$ [46]. The simulation provides a weaker Na–O bond which explains the negative differences associated with the prediction of the Young's modulus for sodium silicate glasses. However, both the simulation and experimental data show that the force constant of the cation mode frequencies increases in the order K < Na < Li, in agreement with the ranking of the elastic constants at a fixed alkali concentration.

Figure 1 shows that Li addition to silica glass leads to an increasing of cross-linking and cohesion of the network. Therefore, the experimentally determined increasing of the elastic constant values with respect to the silica glass is easily explained as a direct consequence of Li induced network polymerization and cohesion.

Because of their higher coordination numbers, longer distances and lower force constants, both Na and K act as purely modifier cations. Their effect on network depolymerization dictates the Young's modulus macroscopic behaviour, with E decreasing more sharply for K, which forms larger rings, as shown in Fig. 1c.

The comparison between NS25 and N15C10S glass shows that the Young's modulus increases when sodium ions are substituted by calcium one. This is a consequence of the stronger Ca–O bond as is shown by the projection of VDOS for Ca reported in Fig. 4. Therefore, Ca ions lead to a more packed structure and increases the cohesion energy of the glass.

3.3 Mechanism of the alkali diffusion process

Figure 5 shows the temperature dependence of the computed diffusion coefficients of alkaline ions in the LS15, NS15 and

KS15 glasses. All the linear fits show a regression factor very close to 1 and the activation energies (AE) increase with increasing cation size and coordination number. The AE values are 58.2±1.3, 65.2±0.3 and 69.7±1.9 kJ/mol for Li, Na and K ions, respectively.

Experimental data obtained by tracer diffusivity yielded similar values. In fact, Beier and Frischat [47] reported for Li in the $18Li_2O \cdot 82SiO_2$ glass AE = 65.6 kJ/mol in the range 580–720 K. Frischat [48] reported for Na in the $14.8Na_2O \cdot 85.2SiO_2$ glass AE = 77 kJ/mol in the range 518–678 K and Evstrop'ev and Pavloskii [49] reported for K in the $15K_2O \cdot 85SiO_2$ glass AE = 80.5 kJ/mol in the range 600–800 K. The results obtained from simulations in this paper underestimate the activation energy of about 10–15%. Conversely, the results obtained by Horbach et al. [50] using constant volume simulations in the range 4,000–2,100 K with the box size fixed at a volume corresponding to the density at room temperature, overestimated the activation energy of soda-silicate glasses of about 20–30%.

Accordingly with previous findings [51,52], the alkali ions jump mechanism seems to be vacancy-like, rather than interstitial-like. The process involves the correlated jump of two cations, M1 and M2. At the start of the process, M1 jumps out of its original site into a site that is originally empty; this is a transition site that M1 occupies only momentarily. Almost simultaneously, M2 begins its jump into the site vacated by M1. At the time that M2 begins its jump into site1, M1 moves out of its temporary home into a third site. This site was occupied at the start of the jump sequence by another M ion, although by the time that M1 is ready to move into that site, it has been vacated. Alkaline ions move inside the percolation channels created by NBOs which are linked to network former ions and waggle to accompany the alkaline jump. When more modifiers are present in the glass, the mixed alkali effect occurs [53]. In glasses containing two different alkali species, a deeper minimum in the mobility of the ions with respect to one of the binary alkaline-silica glass is observed. Even small concentrations of a second alkali species effectively slow down the total ion dynamics. Observations suggested a description of dynamics in terms of stable sites mostly specific to one ionic species. Therefore, the rate slow down was related to the limited accessibility of foreign sites [23].

The temperature dependence of diffusion coefficients of Na ions in the NS25 and N15C10S glasses is reported in Fig. 6. It is clear that the AE of the Na ions increases by increasing the ratio CaO/Na_2O. In fact, the activation energy of Na diffusion increases from 54.5 ± 1.3 kJ/mol for the NS25 glass to 71.4±0.8 kJ/mol for N15C10S glass. This effect can be explained by looking at the graphic visualization of the glass structures in Fig. 3. The Ca ions lie in the percolations channel created by ions modifier (Na and Ca). This agrees with the findings reported by Cormack and Du [40]

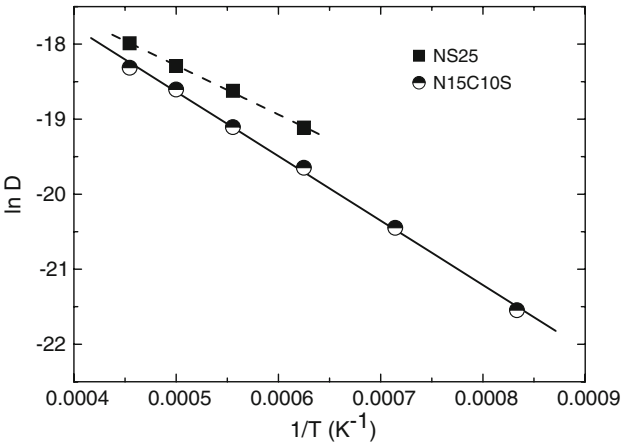

Fig. 6 Arrhenius plots of the diffusion coefficients of Na in NS25 and N15C10S glasses

who studied how the replacement of sodium with calcium changes the structure of soda lime glasses. Calcium was seen to play a similar, modifying, role as sodium in the structure. On substitution, Ca replaces sodium, entering the modifier-rich regions in the glass. Having diffusivities several order of magnitude smaller, Ca ions obstruct the channels and hamper Na diffusion.

4 Conclusions

The combined molecular dynamics simulations and energy minimization study carried out in this work has allowed the correct quantitative evaluation of the Young's modulus of several silicate glasses. The excellent agreement between the simulation results and the experimental data testifies to a prediction performance superior to those of the empirical methods commonly used in the glass scientific community. More importantly, the main advantage of atomistic simulations over empirical methods rests in their ability to deepen the interpretative levels obtained from the experiments by providing atomic pictures of the glass structures and detailed insight into composition–atomic structure relationships. In particular, the balance of two concurrent factors with differing consequences on the glass network seems to be responsible of the compositional dependence of the Young's modulus observed experimentally in the series of glasses studied. These factors are: (1) depolymerization of the silica network that leads to a decrease of the elastic constants; (2) increase of the overall glass cohesion caused by the establishment of alkali–NBO bonds that lead to an increase in the elastic constants as a function of the chemical nature and concentration of the modifiers.

The vacancy-like diffusion mechanisms is found to be similar for the three alkaline ions with the activation energy governed by the ionic dimensions and masses of the alkaline atoms. In soda-lime glasses, the Ca ions act as modifiers contributing to the formation of the percolation channels together with the Na ions. However, because of the differences in valency and strength of bond with oxygens with respect to the Na ions, the Ca ions are less mobile in the structure and tend to hinder *the Na walk* with consequent increase of the activation energy of Na diffusion.

References

1. Henderson GS (1995) J Non-Cryst Solids 183:43
2. Mazzara C, Jupille J, Flank AM, Lagarde P (2000) J Phys Chem B 104:3438
3. Maekawa H, Maekawa T, Kawamura K, Yokokawa T (1991) J Non-Cryst Solids 127:53
4. Voigt U, Lammert H, Eckert H, Heuer A (2005) Phys Rev B 72:64207
5. Dupree R, Holland D, Williams DS (1986) J Non-Cryst Solids 81:185
6. Dupree R, Holland D, Mortuza MG (1990) J Non-Cryst Solids 116:148
7. Sen S, Gerardin C, Navrotsky A, Dickinson JE (1994) J Non-Cryst Solids 168:64
8. Sen S, Youngman RE (2003) J Non-Cryst Solids 331:100
9. Eckert H, Elbert S, Epping JD, Janssen M, Kalwei M, Strojek W, Voigt U (2004) Top Curr Chem 246:195
10. Zhao J, Gaskell PH, Cluckie MM, Soper AK (1998) J Non-Cryst Solids 232:721
11. Hannon AC, Vessal B, Parker JM (1992) J Non-Cryst Solids 150:97
12. Uhlig H, Hoffmann MJ, Lamparter HP, Aldiger F, Bellissent R, Steeb S (1996) J Am Ceram Soc 79:2833
13. Misawa M, Price DL, Suzuki K (1980) J Non-Cryst Solids 37:85
14. Wright AC, Clare AG, Bachra B, Sinclair RN, Hannon AC, Vessal B (1991) Trans Am Crystallogr Asso 27:239
15. Smith W, Greaves GN, Gillian MJ (1995) J Chem Phys 103:3091
16. Yuan X, Cormack AN (2001) J Non-Cryst Solids 283:69
17. Du J, Cormack AN (2004) J Non-Cryst Solids 349:66
18. Du J, Corrales R (2005) Phys Rev B 72:1
19. Du J, Corrales R (2006) J Non-Cryst Solids 352:3255
20. Jund P, Kob WRJ (2001) Phys Rev B 64:134303
21. Banhatti DR, Heuer A (2001) Phys Chem Chem Phys 3:5104–5108
22. Heuer A, Kunow M, Vogel M, Banhatti RD (2002) Phys Chem Chem Phys 4:3185–3192
23. Lammert H, Heuer A (2005) Phys Rev B B72:214202
24. Greaves GN (1985) J Non-Cryst Solids 71:203
25. Varshneya AK (1994) Fundamentals of inorganic glasses. Academic Press, USA
26. SciGlass 3.5; SciVision: Burlington, 1997
27. Smith W, Forester TR (1996) J Mol Graph 14:136
28. Ewald PP (1921) Ann Phys 64:253
29. Pedone A, Malavasi G, Menziani MC, Cormack AN, Segre U (2006) J Phys Chem B 110:11780–11795
30. Gale JD, Rohl AL (2003) Mol Simul 29:291
31. Malavasi G, Pedone A, Menziani MC (2006) Mol Simul 32(10):1–11
32. Malavasi G, Menziani MC, Pedone A, Segre U (2006) J Non-Cryst Solids 352:285
33. Pedone A, Malavasi G, Cormack AN, Segre U, Menziani MC (2007) Chem Mater 19(13):3144–3154
34. Leach AR (2001) Molecular modelling: principle and applications. Prentice-Hall, London
35. Gale JD (2005) GULP manual. Curtin University of Technology
36. Fletcher R, Reeves CM (1964) Comput J 7:149
37. Allen MP, Tildesley DJ (1989) Computer simulation of liquids. Clarendon Press, Oxford
38. Clare AG, Bachra B, Wright AC, Sinclair RN (1992) The physics of non-crystalline solids. Taylor & Francis, London
39. Greaves GN, Fontaine A, Lagrarde P, Raoux D, Gurman SJ (1981) Nature 293:611
40. Cormack AN, Du J (2001) J Non-Cryst Solids 293–295:283–289
41. Lusvardi G, Malavasi G, Menabue L, Menziani MC, Pedone A, Segre U (2005) J Phys Chem B 109:21586
42. Bansal NP, Doremus RH (1986) Handbook of glass properties. Academic Press, Orlando
43. Priven AI (2004) Glass Technol 45:244
44. Vallis Y, Luspin Y, Hauret G (1996) Mater Sci Eng B 40:199
45. Exarhos G, Risen WM Jr (1972) Solid State Commun 11:755
46. Hauret G, Vailles Y, Parot-Rajaona T, Gervais F, Mas D, Luspin Y (1995) J Non-Cryst Solids 191:85
47. Beier W, Frischat GH (1980) J Non-Cryst Solids 38/39:569
48. Frischat GH (1975) Cent Glass Ceram Res Inst Bull 22:129
49. Estrop'ev KK, Pavloskii VK (1967) Inorg Matter 3:592
50. Horbach J, Kob W, Binder K (2001) Chem Geol 174:87–101
51. Cormack AN, Du J, Zeitler TR (2002) Phys Chem Chem Phys 4:3193–3197
52. Smith W, Forester TR, Greaves GN, Hayter S, Gillan MJ (1997) J Mater Chem 7:331–336
53. Rolling B, Ingram MD (1998) Solid State Ionics 105:47
54. Manghnani MH (1986) In: Bansal NP, Doremus RH (eds) Handbook of glass properties. Academic Press, London
55. Hwa LG, Hsieh KJ, Liu LC (2003) Mater Chem Phys 78:105
56. Wilantewicz T (1998) The effects of lithium, boron, and magnesium oxides on the mechanical properties of silicate glasses. Alfred University, Alfred